Received: 22 August 2017 | Revised: 26 March 2018 | Accepted: 27 March 2018

DOI: 10.1111/gcb.14274

PRIMARY RESEARCH ARTICLE

WILEY Global Change Biology

Joint structural and physiological control on the interannual variation in productivity in a temperate grassland: A data-model comparison

Zhongmin Hu[1,2,3,#] | Hao Shi[4,#] | Kaili Cheng[2,3] | Ying-Ping Wang[5,6] | Shilong Piao[7,8] | Yue Li[7] | Li Zhang[2,3] | Jianyang Xia[9,10] | Lei Zhou[11] | Wenping Yuan[12] | Steve Running[13] | Longhui Li[14] | Yanbin Hao[15] | Nianpeng He[2,3] | Qiang Yu[3,4,16] | Guirui Yu[2,3]

[1]School of Geography, South China Normal University, Guangzhou, China

[2]Synthesis Research Center of Chinese Ecosystem Research Network, Key Laboratory of Ecosystem Network Observation and Modeling, Institute of Geographic Sciences and Natural Resources Research, Chinese Academy of Sciences, Beijing, China

[3]College of Resources and Environment, University of Chinese Academy of Sciences, Beijing, China

[4]State Key Laboratory of Soil Erosion and Dryland Farming on the Loess Plateau, Northwest A & F University, Yangling, China

[5]CSIRO Oceans and Atmosphere, Aspendale, Vic., Australia

[6]Terrestrial Biogeochemistry Group, South China Botanic Garden, Chinese Academy of Sciences, Guangzhou, China

[7]Sino-French Institute for Earth System Science, College of Urban and Environmental Sciences, Peking University, Beijing, China

[8]Institute of Tibetan Plateau Research, Chinese Academy of Sciences, Beijing, China

[9]Tiantong National Forest Ecosystem Observation and Research Station, School of Ecological and Environmental Sciences, East China Normal University, Shanghai, China

[10]Institute of Eco-Chongming (IEC), Shanghai, China

[11]College of Geography and Environmental Sciences, Zhejiang Normal University, Jinhua, China

[12]School of Atmospheric Sciences, Sun Yat-Sen University, Guangzhou, China

[13]NTSG, College of Forestry and Conservation, University of Montana, Missoula, Montana

[14]School of Geographic Science, Nanjing Normal University, Nanjing, China

[15]College of Life Sciences, University of Chinese Academy Sciences, Beijing, China

[16]School of Life Sciences, University of Technology Sydney, Sydney, NSW, Australia

Abstract

Given the important contributions of semiarid region to global land carbon cycle, accurate modeling of the interannual variability (IAV) of terrestrial gross primary productivity (GPP) is important but remains challenging. By decomposing GPP into leaf area index (LAI) and photosynthesis per leaf area (i.e., GPP_leaf), we investigated the IAV of GPP and the mechanisms responsible in a temperate grassland of northwestern China. We further assessed six ecosystem models for their capabilities in reproducing the observed IAV of GPP in a temperate grassland from 2004 to 2011 in China. We observed that the responses to LAI and GPP_leaf to soil water significantly contributed to IAV of GPP at the grassland ecosystem. Two of six models with prescribed LAI simulated of the observed IAV of GPP quite well, but still

[#]The authors contributed equally to this manuscript.

Correspondence
Zhongmin Hu, School of Geography, South China Normal University, Guangzhou, China.
Email: huzm@m.scnu.edu.cn
and
Hao Shi, State Key Laboratory of Soil Erosion and Dryland Farming on the Loess Plateau, Northwest A & F University, Yangling, China.
Email: Hao.Shi@student.uts.edu.au

Funding information
National Key R&D Program of China, Grant/Award Number: 2017YFA0604801; National Natural Science Foundation of China, Grant/Award Number: 31570437, 41730645, 41371119; Startup Foundation for Talented Scholars in South China Normal University, Grant/Award Number: S82360, A314021403-C4, A314021402-1703; Youth Innovation Research Team Project of LENOM, CAS, Grant/Award Number: LENOM2016Q0004; Youth Innovation Promotion Association, CAS, Grant/Award Number: 2015037; Special-Funds of Scientific Research Programs of State Key Laboratory of Soil Erosion and Dryland Farming on the Loess Plateau, Grant/Award Number: S82360, A314021403-C4, A314021402-1703; Special-Fund of talents (Thousand Talents Program) in Northwest A&F University, Grant/Award Number: S82360, A314021403-C4, A314021402-1703

underestimated the variance of GPP_leaf, therefore the variance of GPP. In comparison, simulated pattern by the other four models with prognostic LAI differed significantly from the observed IAV of GPP. Only some models with prognostic LAI can capture the observed sharp decline of GPP in drought years. Further analysis indicated that accurately representing the responses of GPP_leaf and leaf stomatal conductance to soil moisture are critical for the models to reproduce the observed IAV of GPP_leaf. Our framework also identified that the contributions of LAI and GPP_leaf to the observed IAV of GPP were relatively independent. We conclude that our framework of decomposing GPP into LAI and GPP_leaf has a significant potential for facilitating future model intercomparison, benchmarking and optimization should be adopted for future data-model comparisons.

KEYWORDS
data-model comparison, ecosystem models, grassland, gross primary productivity, interannual variability

1 | INTRODUCTION

Arid and semiarid regions cover *ca*. 40% of global land surface area (Safriel & Adeel, 2005). Ecosystems in these regions are fragile and sensitive to climate variation (Rotenberg & Yakir, 2010). A previous study showed that fluctuations in carbon uptake by these ecosystems as a result of climate variation played an important role in global carbon cycle and carbon-climate feedback (Ahlstrom et al., 2015). Given such an importance of arid and semiarid ecosystems and projected more frequent and severe extreme climate events (Dai, 2013; Huang, Guan, & Ji, 2012) associated with the shifts in precipitation regimes (Craine & Brunsell, 2012; Wilcox, Fischer, Muscha, Petersen, & Knapp, 2015) in the future, accurate prediction of the responses of carbon balance in semiarid ecosystems to climatic variations is critical for improving predictions of future land carbon cycle and climate change.

Ecosystem and land surface models are commonly used for diagnosing and predicting ecosystem functioning in a changing climate (Cramer et al., 2001; Friedlingstein et al., 2006). However, there are still large uncertainties in model estimates of carbon balance, largely as a result of biases in modeled processes, such as carbon allocation (e.g., Haverd et al., 2016; Restrepocoupe et al., 2016), CO_2 fertilization effect (e.g., Piao et al., 2013; Smith et al., 2016), nutrient limitations (e.g., Agren, Wetterstedt, & Billberger, 2012; Reich et al., 2006), and soil water stress on vegetation (e.g., De Kauwe et al., 2015; Luo, Liang, & Mccarthy, 2013). For example, the estimated global land gross primary productivity (GPP) by CMIP5 models varied 90–210 Gt C/year over the present period (Li et al., 2018; Prentice, Liang, Medlyn, & Wang, 2015). Specifically, at the global scale, carbon balance in semiarid ecosystems is mainly associated with GPP variations resulting from circulation-driven variations of precipitation (Ahlstrom et al., 2015). Therefore, it is necessary to first analyze modeled primary productivity, a key component determining ecosystem carbon balance, for understanding the modeled response of net ecosystem productivity (NEP) to climate drivers in semiarid ecosystems, in particular at the interannual time-scale.

To reduce model uncertainties in simulating carbon cycle, the modeling community has made great efforts in benchmarking models against observations at various spatio-temporal scales (e.g., Best et al., 2015; Luo et al., 2012). Some frameworks are proposed to identify key processes underlying the intermodel divergence through decomposing a target model output into a number of component variables, each of which represents a subset of underlying processes (Xia, Luo, Wang, & Hararuk, 2013; Zaehle et al., 2014). For example, ecosystem net primary productivity has been decomposed as the product of nitrogen use efficiency and nitrogen uptake (Zaehle et al., 2014) or the product of carbon use efficiency and GPP (Xia et al., 2017) in evaluating terrestrial ecosystem models. However,

difficulties exist with these frameworks because the components usually interact with each other and those interactions often are difficult to be observed and quantified (e.g., nitrogen use efficiency).

In order to identify key processes determining the interannual variations in ecosystem GPP of a temperate grassland, here we propose a top-down component analysis framework (Figure 1) that decomposes GPP into two contributing components: leaf area index (LAI) and the ratio of GPP over LAI (GPP/LAI, hereafter GPP_leaf). LAI and GPP_leaf represent structural and physiological contributions to vegetation productivity respectively. LAI is generally determined by the fraction of carbon assimilate allocated to leaf (Murray-Tortarolo et al., 2013; Restrepocoupe et al., 2016) while GPP_leaf is determined mostly by the leaf-scale net photosynthesis (A_n). GPP_leaf is largely regulated by two physiological factors, namely maximum RuBP carboxylation rate, V_{cmax}, and stomatal conductance, g_s (Figure 1). Both V_{cmax} and g_s vary significantly with available soil water, particularly in semiarid ecosystems. This framework facilitates comparison of model simulations directly with observations without derivations. In addition, the processes affecting LAI and GPP_leaf are relatively independent, which is helpful for benchmarking ecosystem models and identifying key model uncertainties.

In this study, we compared the observed interannual variations in GPP with the modeled by six ecosystem models at a temperate grassland site. Using the framework mentioned above, i.e., decomposing GPP into LAI and GPP_leaf, we compared modeled LAI and GPP_leaf with the observed. The objectives of this study are to (1) quantify how changes in precipitation, especially droughts, affected the interannual variability in GPP at the grassland ecosystem, (2) test whether the models can capture the observed interannual variability in GPP, especially the GPP reductions in drought years, (3) ascertain which component, i.e., LAI or GPP_leaf, contributes to the model's failure to capture the GPP variation, and (4) identify the key model assumptions leading to the bias between models and observations.

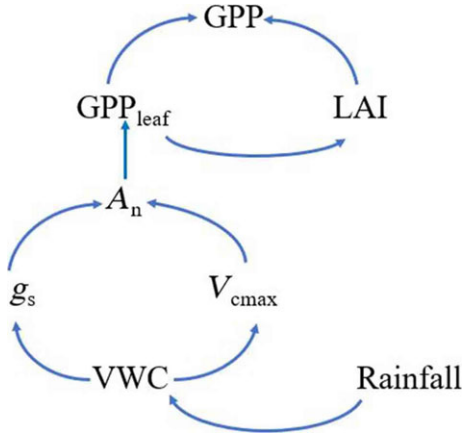

FIGURE 1 An illustration of the hierarchical processes that control the responses of vegetation productivity to rainfall in a temperate grassland. Rainfall recharges volumetric soil water content (VWC), while VWC affects leaf net photosynthesis (A_n) through regulating the maximum RuBP carboxylation rate (V_{cmax}) and leaf stomatal conductance (g_s). A_n is the major determinant of gross primary productivity (GPP) per leaf area (GPP_leaf). At the canopy level, GPP is codetermined by GPP_leaf (a physiological factor) and leaf area index (LAI, a structural factor) [Colour figure can be viewed at wileyonlinelibrary.com]

2 | MATERIALS AND METHODS

2.1 | Site and measurements

The site is located at the Xilingol temperate grassland ecosystem research station (44°33′N, 116°40′E, hereafter CN-Nmg) in Inner Mongolia in northwestern China, with an elevation of 1,190 m. The grassland ecosystem is water-limited, and experienced several droughts during 2004–2011 (Guo et al., 2015). From 1982 to 2003, the mean annual surface air temperature is −0.4°C and the mean annual precipitation is 350 mm, of which approximately 80% falls during the growing season when >95% of annual GPP is produced (May-September, i.e., DOY 120-270). The dominant species are *Leymus chinesis*, *Stipa grandis*, and *Agropyron cristatum* with an average canopy height of 0.5 m and a maximum leaf area index of 1.5 m^2/m^2 (Hu et al., 2008). The soil texture is medium loam (8%/90%/2% for sand/silt/clay), and the average surface bulk density (0–10 cm) is 1.20 g/cm^3.

An eddy covariance (EC) system was mounted onto a tower at a height of 1.5 m, consisting of a three-dimensional sonic anemometer (Model CSAT3, Campbell Scientific Inc., Logan, UT, USA) and a CO_2/H_2O analyzer (Model LI-7500, Li-Cor Inc., NE, USA). Meteorological variables, such as air temperature, precipitation, global radiation and relative humidity, and volumetric soil water content (VWC) at the depths of 5, 20, and 40 cm were collected at a half-hourly time-step. Quality control and gap-filling were performed according to the standard ChinaFlux processing method (Yu et al., 2006). GPP was calculated as the sum of NEP and ecosystem respiration (R_{eco}) with the latter derived from the relationship between nighttime NEP and soil temperature and soil water content. The energy balance ratio during 2004–2011 ranged from 0.81 to 1.07, suggesting good quality of EC measurements (Figure S1).

To obtain a LAI for the site, we estimated LAI with MODIS NDVI (8-day, 250 m) via an exponential function established at the same site ($LAI = 0.106e^{4.064NDVI}$, $R^2 = .94$) and used this function and NDVI data to estimate the daily LAI of the entire growing seasons (Hu et al., 2009). To establish this function, LAI was measured by harvesting the live leaves of aboveground biomass at six 1×1 m^2 quadrats and measuring the leaf area with the scanning method at 2-week intervals in the growing seasons of 2003–2006 (Hao et al., 2010).

2.2 | Terrestrial ecosystem models

Six process models were used in this study, including BEPS (Chen, Liu, Cihlar, & Goulden, 1999), Biome-BGC (Thornton et al., 2002), CABLE (Wang et al., 2011), CLM (Oleson et al., 2010), ORCHIDEE (Krinner et al., 2005), and TECO (Weng & Luo, 2008). The key processes of primary productivity are listed in Table 1.

TABLE 1 Summary of key processes for simulating gross primary productivity in the six models

Model	BEPS	Biome-BGC	CABLE
Version	Original	4.2	2.0b
Time-step	Daily	Daily	30-min
Photosynthesis	Farquhar et al. (1980) $A_n = (C_a - C_i)g_s$	Farquhar et al. (1980) $A_n = (C_a - C_i)g_s$	Collatz et al. (1991); Collatz, Ribascarbo, and Berry (1992) $A_n = (C_a - C_i)g_s$
V_{cmax}	$V_{c\max} = V_{c\max,25}2.4^{(T_{day}-25)/10}f(T_{day})f(N)$	$V_{c\max} = \varepsilon_{25}N_aF_{LNR}F_{NR}\frac{1.8Q_{10\varepsilon}^{(T_{day}-15)/10}}{Q_{10\varepsilon}}$	$V_{c\max} = V_{c\max,25}f(T_v)$ V_{cmax} is then scaled from leaf to canopy using a radiation function.
Stomatal conductance	$g_s = \max(g_{s\max}f(\mathrm{PPFD})f(T_{day})f(D)f(\theta_s), g_0)$ $f(\theta_s) = \sum w_i f_{r,i}$ $w_i = \begin{cases} 0.05, \theta_i \le \theta_{wilt} \\ 2\frac{\theta_i - \theta_{wilt}}{\theta_{fc} - \theta_{wilt}} - \left(\frac{\theta_i - \theta_{wilt}}{\theta_{fc} - \theta_{wilt}}\right)^2, \theta_{wilt} < \theta_i < \theta_{fc} \\ 1 - 0.4\frac{\theta_i - \theta_{fc}}{\theta_{sat} - \theta_{fc}}, \theta_i \ge \theta_{fc} \end{cases}$	$g_s = g_{s\max}f(\mathrm{PPFD})f(T_{min})f(D)f(\psi_s)$ $f(\psi_s) = \begin{cases} 0, \psi_s \le \psi_{s\min}(-2.3) \\ \frac{\psi_s - \psi_{s\min}}{\psi_{s\max} - \psi_{s\min}}, \psi_{s\min} < \psi_s < \psi_{s\,max} \\ 1, \psi_s \ge \psi_{s\max}(-0.6) \end{cases}$	$g_s = g_0 + \frac{g_1 f_w A_n}{(C_a - \Gamma)(1 + D/D_0)}$ $f_w = \min\left(1.0, \max\left(\left(\frac{\theta_i - \theta_{wilt}}{\theta_{sat}}\right)^{\frac{\gamma}{\theta_i - \theta_{wilt}}}\right)\right)$
Canopy model	One layer two-leaf model	One layer two-leaf model	One layer two-leaf model
Soil water model	Three-layer diffusion type	One-layer bucket type	Six-layer diffusion type
Root distribution	Root biomass fraction is parameterized by Jackson et al. (1996) as $\sum_{i=1}^{n} f_{r,i} = 1 - \beta_r^{z_n}$ with $\beta r = 0.943$ for temperate grasslands	NA	Root biomass fraction is parameterized by Jackson et al. (1996) as $\sum_{i=1}^{n} f_{r,i} = 1 - \beta_r^{z_n}$ with $V_{c\max} = V_{c\max,opt}f(T_v)$ for temperate grasslands
Root water uptake	$f(f_{r,i}, \theta_i)$	NA	$f(K_r, K_s, f_{r,i}, \theta_i)$
LAI	Prescribed	Leaf growth occurs at a daily time-step, calculated as a fixed fraction of available carbon allocation scaled by available nitrogen. Grass phenology is a function of degree-day summation and annual precipitation summation. The actual leaf onset is 15 days prior to the estimation by the above method. On leaf onset, the storage pool in previous year is used for sprouts. Daily LAI is then determined by leaf carbon and a constant SLA.	Prescribed
Reference	Chen et al. (1999)	White, Thornton, Running, and Nemani (2000)	Kowalczyk, Wang, and Law (2006); Wang et al. (2011)
Model	**CLM**	**ORCHIDEE**	**TECO**
Version	4.0	Original	Original
Time-step	30-min	30-min	Hourly
Photosynthesis	Collatz et al. (1991, 1992) $A_n = (C_a - C_i)g_s$	Farquhar et al. (1980) for C3; Collatz et al. (1992) for C4 $A_n = (C_a - C_i)g_s$	Farquhar et al. (1980) $A_n = (C_a - C_i)g_s$

(Continues)

TABLE 1 (Continued)

Model	CLM	ORCHIDEE	TECO
V_{cmax}	$V_{c\,max} = V_{c\,max,25} 2.4^{(T_v-25)/10} f(T_v)\beta_t f(DYL)$ $V_{c\,max.25} = \varepsilon_{25} N_a F_{LNR} F_{NR}$ $\beta_t = \sum w_i f_{r,i}$ $w_i = \begin{cases} 0, T_i \le T_f \\ \frac{\psi_{s\,min} - \psi_{s,i}}{\psi_{s\,min} + \psi_{ssat,i}}, T_i > T_f \end{cases}$	$V_{c\,max} = V_{c\,max,opt} e_{rel}(a_{rel}) f_w$ $f_w = \begin{cases} 0, \theta \le \theta_{wilt}(0.028) \\ 1 - \frac{\theta - \theta_{wilt}}{\theta_{sat} - \theta_{wilt}}, \theta_{wilt} < \theta < \theta_{crit} \\ 1, \theta \ge \theta_{crit}(0.5) \end{cases}$	$V_{c\,max} = V_{c\,max,opt} f(T_v)$
Stomatal conductance	$g_s = g_0 + \frac{g_1 A_n h_r}{C_a}$	$g_s = g_0 + \frac{g_1 A_n h_r}{C_a}$	$g_s = g_0 + \frac{g_1 f_w S_{NSC} A_n}{(C_a - \Gamma)(1 + D/D_0)}$ $f_w = \sum w_i f_{rl}$, i $w_i = \frac{\theta_i - \theta_{wilt}}{\theta_{fc} - \theta_{wilt}}$
Canopy model	One layer two-leaf model	Big leaf model	One layer two-leaf model
Soil water model	Multiple-layer diffusion type	11-layer diffusion type	10-layer diffusion type
Root distribution	Root fraction in each soil layer depends on plant functional type and is as $\left\{ \begin{array}{l} f_{r,i} = 0.5(e^{-r_a z_{i-1}} + e^{-r_b z_{i-1}} - e^{-r_a z_i} \\ -e^{-r_b z_i}), 1 \le i < n \\ 0.5(e^{-r_a z_{i-1}} + e^{-r_b z_{i-1}}), i = n \end{array} \right\}$ with r_a being 11.0 and r_b being 2.0 for C3 grass	Root density profile decreases exponentially with soil depth, and is parameterized as $f_{rl,i} = e^{-z_i/\zeta}$ with ζ = 1.5 m for trees and ζ = 0.3 m for grasses	Rooting depth is 70 cm and reaches the fourth soil layer with initial ratios of roots as 40% (0~10 cm), 40% (10~30 cm), 15% (30–50 cm), and 5% (50~70 cm)
Root water uptake	$f(K_r, K_s, f_{r,i}, \theta_i)$	$f(K_r, K_s, f_{r,i}, \theta_i)$	$f(K_r, K_s, f_{r,i}, \theta_i)$

(Continues)

TABLE 1 (Continued)

Model	CLM	ORCHIDEE	TECO
LAI	Leaf growth occurs at a half-hourly time-step, depending on GPP, maintenance respiration and the carbon allometric relationship between new leaf carbon, new stem carbon and new fine and coarse root carbon, and available nitrogen. The seasonal deciduous phenology algorithm is the same as Biome-BGC for grasslands. LAI is then calculated by leaf carbon and a SLA changing linearly along a vertical canopy gradient. On leaf onset, LAI in the new year can initiate rapid growth using storage carbon and nitrogen.	The fractions of carbon allocation to compartments are parameterized as a function of moisture, temperature and nitrogen availabilities at a half-hourly time-step. The leaf onset for temperate grass is determined by a simple growing degree-day criterion, while leaf senescence is determined by the combination of temperature and soil water availability. On leaf onset, carbon reserve in the previous year is used to grow a minimum quantity of leaves and roots. LAI is then calculated by leaf carbon and a constant SLA. When LAI is higher a prescribed maximum value, no leaf growth occurs.	Leaf growth occurs at a daily time-step, calculated as a constant relative ratio of leaf biomass scaled by daily temperature, soil water content and non-structural carbon storage. The phenology is determined by growing degree days (GDD) above 5°C. Leaf onset for grass occurs when GDD > 600 and carbon storage in the previous year is used for initial growth. Daily LAI is then determined by leaf carbon and a constant SLA.
Reference	Oleson et al. (2010); Thornton and Zimmermann (2007)	Krinner et al. (2005)	Weng and Luo (2008)

C_a and C_i are atmospheric and intercellular CO_2 concentration, respectively; $V_{cmax,25}$ is the maximum rate of RuBP carboxylation at 25°C; $f(T_{day})$ in V_{cmax} formula is a function describing the effect of mean daily temperature (T_{day}) on V_{cmax}; $f(N)$ is a function describing the effect of nitrogen on V_{cmax}; $Q_{10\varepsilon}$ is the sensitivity of the activity of Rubisco (ε) per 10°C change in temperature; T_v is the leaf temperature; β_t ($0 \sim 1$) is the soil water stress on V_{cmax} as a function of the soil water potential and root distribution in each soil layer; DYL is the daytime length; ε_{25} is the activity of Rubisco at 25°C; N_a is the area-based leaf nitrogen concentration; F_{LNR} is the fraction of leaf nitrogen in Rubisco; F_{NR} is the fraction of nitrogen in Rubisco molecular mass; $V_{cmax,opt}$ is the maximum rate of RuBP carboxylation at PFT-dependent optimum temperature; e_{rel} is the relative photosynthetic efficiency as a function of the relative leaf age a_{rel}, which is defined as the ratio of the leaf age over the PFT-dependent mean leaf life-time; g_s is stomatal conductance; g_{smax} is the maximum stomatal conductance depending on PFTs; g_0 is the residual stomatal conductance when the net assimilation rate (A_n) is zero; g_1 represents the sensitivity of stomatal conductance to assimilation, ambient CO2 concentration and environmental controls; PPFD is photosynthetic photon flux density; $f(T_{day})$ in calculating g_s is a function describing the effect of temperature on g_s; $f(D)$ is a function describing the effect of vapor pressure deficit (D) on g_s; f_w is a function describing the soil water stress on stomatal conductance and w_i is the soil water stress from soil layer i; $f_{r,i}$ and $f_{rl,i}$ are the fraction of root biomass and root length in soil layer i, respectively; n is the number of soil layers; z_i is the depth of soil layer i; r_a and r_b are plant-dependent root distribution parameters; β_r is the extinction coefficient for vertical root biomass distribution; T_i is the temperature in soil layer i and T_f is the freezing temperature; θ_i is soil water content in soil layer i; θ_{wilt}, θ_{fc} and θ_{sat} are soil wilting point, saturated soil water content and field capacity, respectively; Ψ_s is the soil water potential (MPa/mm) and Ψ_{ssat} is the saturated water potential; Ψ_{smin} and Ψ_{smax} are soil water potentials when stomata is fully closed and open, respectively; T_{min} is the minimum daytime temperature; Γ is the CO_2 compensation point; D_0 is an empirical constant; h_r is relative humidity at the leaf surface; P_a is atmospheric air pressure; S_{NSC} is a scaling factor derived by the size of nonstructural pool; K_r is hydraulic productivity of roots; K_s is soil hydraulic conductivity; $f(K_r, K_s, f_{r,i}, \theta_i)$ is a function for deriving root water uptake from soil.

All models adopt a biochemical model of photosynthesis coupled with stomatal conductance to calculate net carbon assimilation. The net photosynthesis, A_n, is calculated following Farquhar, Von Caemmerer, and Berry (1980) as the minimum of Rubisco-limited and light-limited potential capacities, or Collatz, Ball, Grivet, and Berry (1991) assuming a third limitation on A_n by the rate of export or utilization of the photosynthesis products. As a key parameter determining A_n, V_{cmax} is estimated differently among the six models, but in general as a function of leaf nitrogen concentration, leaf age, air temperature, or soil water (Table 1). Plant stomatal conductance, g_s, which is another key variable determining leaf photosynthesis, is estimated in two ways. The first (e.g., BEPS and Biome-BGC) down-regulates a maximum stomatal conductance by environmental constraints, including photosynthetic photo flux density (PPFD), air temperature (T_a), vapor pressure deficit (VPD), and soil water potential (Ψ_s) etc. (e.g., Jarvis, 1976). The second (e.g., CABLE, CLM, ORCHIDEE, and TECO) adopts the Ball-Berry model or its variants to relate g_s and A_n through a semiempirical function consisting of environmental factors, e.g., air relative humidity or VPD, and soil water content (Ball, Woodrow, & Berry, 1987; Leuning, 1995). It is noted that four models, BEPS, Biome-BGC, CABLE and TECO, explicitly consider soil water stress ($f(\theta_s)$, $f(\Psi_s)$ or f_w) on g_s but not on V_{cmax}, whereas CLM and ORCHIDEE include no explicit soil water constraint on g_s but on V_{cmax}.

Prescribed daily LAI is used for BEPS and CABLE but prognostic LAI for other models, which estimate LAI with leaf biomass and a constant parameter, specific leaf area (SLA). Except ORCHIDEE, all the models use the scheme of sunlit and shaded leaves to calculate canopy level photosynthesis. The models differ significantly in characterizing soil water profile, number of soil layers, distribution of root density, and dependence of soil water uptake on soil water and root density (Table 1).

2.3 | Data-model comparison

To ensure the model outputs comparable, we set out a protocol before running the models: (1) all models use the same site information, including meteorological driving forcing (air temperature, precipitation, wind speed, solar radiation, vapor pressure deficit, and surface atmospheric pressure at daily or hourly time-scale), and daily leaf area index (if necessary) as inputs; (2) all models use model-specific default parameters except soil texture, C:N ratios of leaf, root and litter (16, 34, 37), SLA (25 m^2/kg), and spin up using meteorological forcing during 2004–2011; (3) models outputs includes GPP, ET, LAI (if not prescribed), VWC in the first 30 cm of soil depth, V_{cmax}, and leaf stomatal conductance (both shaded and sunlit leaves).

Except calculating the sum for GPP, mean daily LAI, GPP_leaf and VWC in 0–30 cm over the growing season (May to September, i.e., DOY 120-270) were calculated as annual values for both the observations and model outputs. To identify the primary component influencing the observed interannual variability in GPP, the three variables (GPP, LAI, and GPP_leaf) were regressed against corresponding interannual changes in environmental variables respectively. After doing this, model simulations were compared with observations to investigate whether models can reproduce the interannual variations of GPP, LAI, and GPP_leaf, particularly in drought years. The modeled responses of GPP, LAI, and GPP_leaf to environmental factors (especially VWC) were further examined at both the daily and annual time-scales. At the daily time-scale, only data during the peak growing season (Day 180–200) when LAI was relatively constant were used to exclude the influence of LAI. For models using the two-leaf scheme to estimate canopy level fluxes, we used sunlit-leaf g_s and V_{cmax} for analysis, because of the dominant contribution to ecosystem GPP by sunlit leaf.

3 | RESULTS

3.1 | Interannual variations in GPP and relevant variables

Observations showed that the ecosystem experienced significant precipitation deficits in the growing seasons of 2005 and 2009, resulting in drastic reductions of GPP, particularly in 2009 (Figure 2). In addition to GPP, both LAI and ET decreased in the drought years, but the degrees of reduction were less than that of GPP. For example, compared with a mean reduction in 66.9% for GPP, ET, and LAI showed relatively small reductions (28.9% and 26.4%) in the drought years compared with the other years (Figure 2b).

Further analysis showed that interannual variation in GPP was significantly correlated with soil water content ($R^2 = .65$, $p < .05$, Figure 3), but not with other environmental variables, e.g., air temperature (Figure S2) and VPD (Figure S3). For the two components, both GPP_leaf and LAI showed significant positive correlation with VWC (Figure 3, $p < .05$). In comparison, the R^2 of LAI (.42) was apparently smaller than that of GPP_leaf (0.82). This suggests that changes in GPP_leaf contributed more to the interannual variations in GPP than LAI.

3.2 | Data-model comparison of the determinants of GPP variations

As compared with the observed annual GPP, the modeled GPP by the six models all have different biases (Figure 4). The two models with observed LAI as inputs (i.e., BEPS and CABLE) captured the observed interannual variations in GPP with VWC quite well. The R^2 between observed and modeled GPP were as large as .92 and .86 for BEPS and CABLE, respectively ($p < .01$), which were better than the performance of other four models with prognostic LAI. This indicates that LAI is critical for models to simulate the interannual variations in GPP accurately at the study site. However, at the same time, both BEPS and CABLE underestimated the GPP interannual variability. For example, the coefficient of variation (CV) of the simulated GPP by BEPS and CABLE was 0.20 and 0.15, respectively, which was >60% lower than the CV of GPP derived from eddy covariance system (0.49). The key reason for the underestimation by

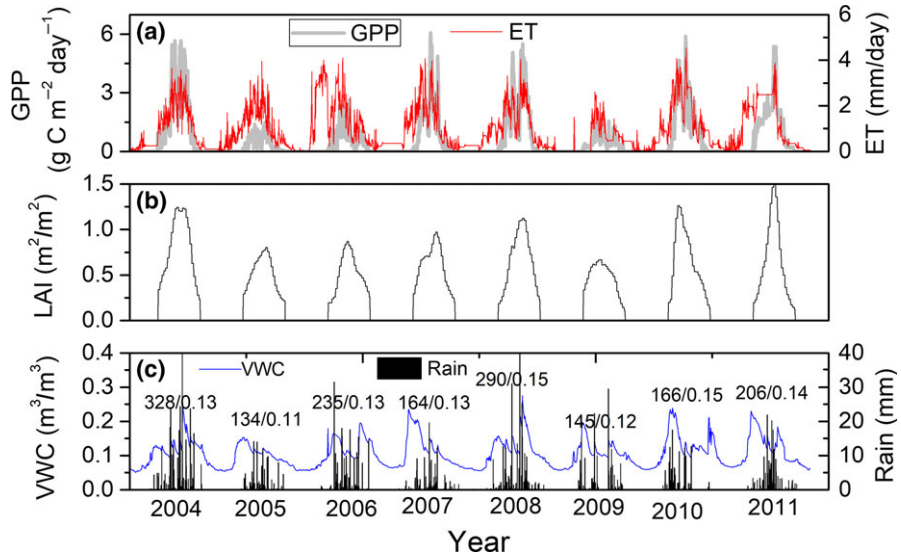

FIGURE 2 Observations of (a) daily GPP and evapotranspiration (ET), (b) LAI, (c) VWC in the top 0–30 cm soil and precipitation at the temperate grassland site from 2004 to 2011. Numbers in (c) are the annual GPP in g C m^{-2} year^{-1} and average VWC in fraction by volume during the growing season of each year (May-September, DOY 120-270) [Colour figure can be viewed at wileyonlinelibrary.com]

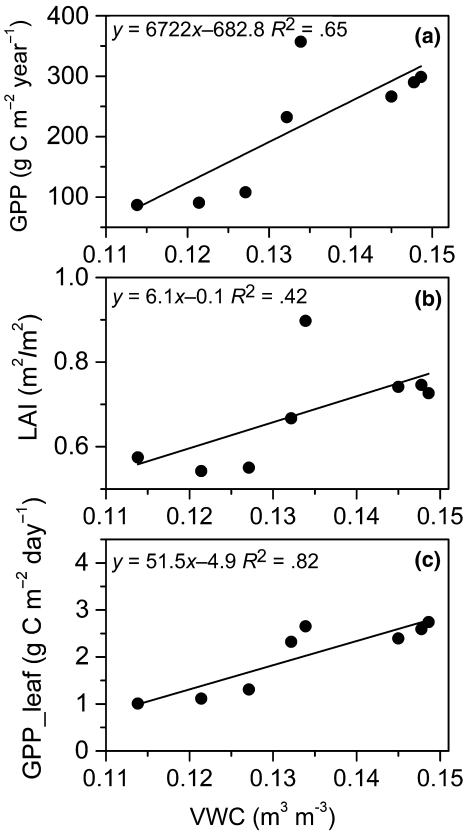

FIGURE 3 Correlations between average daily VWC in the top 0–30 cm soil with (a) annual GPP, (b) mean daily LAI, and (c) mean daily GPP_leaf of the growing seasons from 2004 to 2011

the two models is that the estimated interannual varations of GPP_leaf were much lower than the observation (Figure 4e,f).

The four remaining models with prognostic LAI (i.e., Biome-BGC, CLM, ORCHIDEE, and TECO) simulated the interannual variations in GPP poorly (Figure 4a). No significant correlation was found between the modeled and observed GPP for the four models (Figure 4b). The dominant source of the unsatisfactory performance is that all the models failed to reproduce the observed interannual variation in LAI. Further analysis indicated that the modeled LAI by all these four models were not significantly correlated with the observed (Figure 4d, $p > .05$). In particular, none of the four models correctly captured the observed large reduction in canopy LAI in two drought years (2005 and 2009).

Although the four models generally simulated GPP poorly due to the failure of reproducing the interannual variations in LAI, three models, Biome-BGC, CLM, and ORCHIDEE correctly captured the observed reductions in GPP in two drought years (i.e., 2005 and 2009) (see Figure 4a). Further analysis indicates that simulated GPP_leaf by the three models were significantly correlated with the measurements ($p < .05$, Figure 4f), which contributed to the success in capturing the interannual variation in the observed GPP by these three models over the other models.

Observations illustrated a predominant role of soil water content on the interannual variations in GPP, highlighting the importance of accurate estimate of VWC. Our results indicated that none of the six models were able to reproduce the observed VWC of the whole growing season (Figure S4, $p > .05$). However, over the period of July to August, during which the total GPP contributed on average 56% of annual GPP (the R^2 of the relationship between annual GPP and GPP in July-August was as high as .96), Biome-BGC ($R^2 = .63$), CLM ($R^2 = .41$), and ORCHIDEE ($R^2 = .90$) captured the interannual variations in VWC quite well (Figure 5, $p < .05$). This indicates that the three models captured the reductions in GPP in drought years because they reproduced the observed VWC-GPP relationship well. For other models with prognostic LAI (e.g., TECO), it would be difficult to reproduce the interannual variations in GPP because of the poor performance in predicting the interannual variations of VWC.

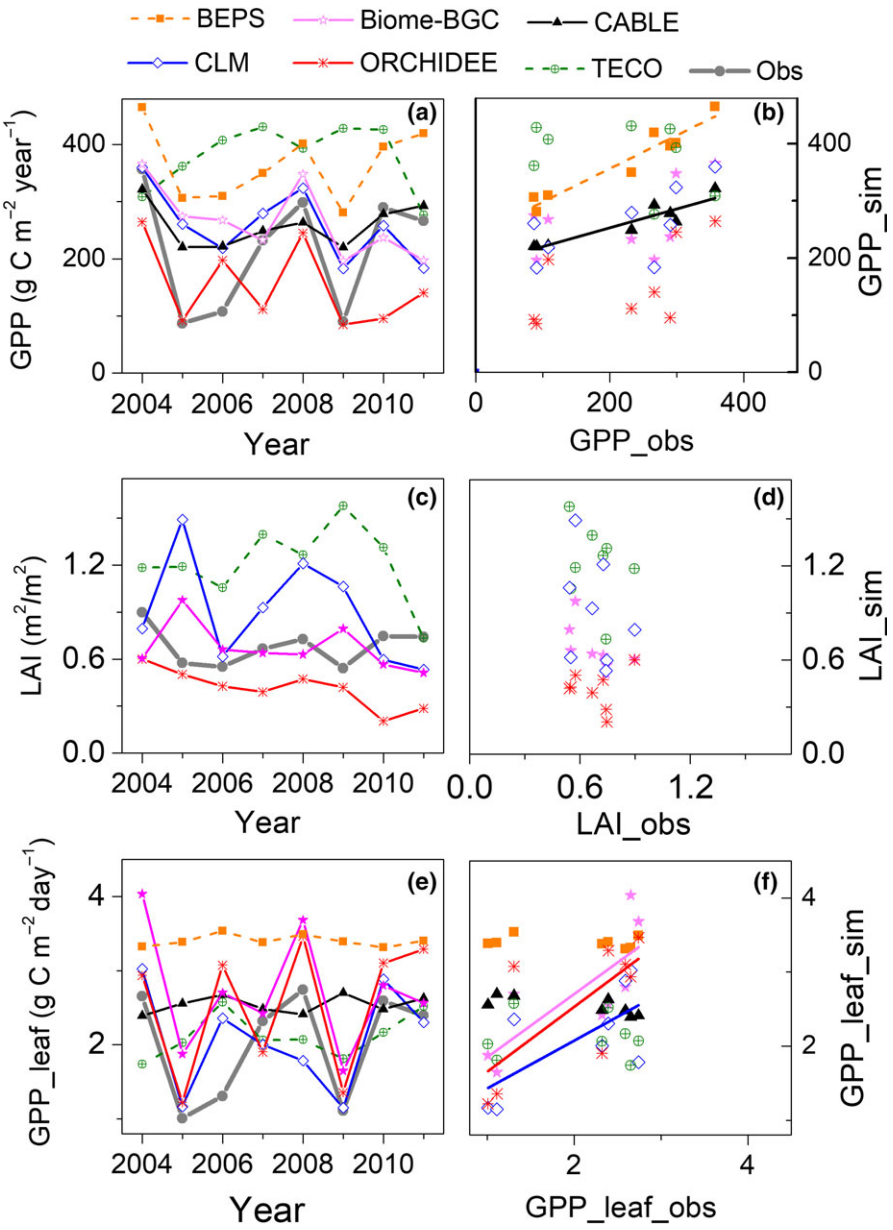

FIGURE 4 Comparison of modeled annual GPP (a, b), LAI (c, d), and GPP_leaf (e, f) with observations. BEPS and CABLE used prescribed LAI as input and thus are not shown in the LAI comparison. In (b) and (f), only the fitted lines that are statistically significant at the level of 0.05 are shown [Colour figure can be viewed at wileyonlinelibrary.com]

3.3 | Simulations of water constraints on GPP, LAI, and GPP_leaf

In addition to capturing the VWC variations during critical growing periods (July-August), the three models (i.e., Biome-BGC, CLM, and ORCHIDEE) also captured the correlation between soil water content and GPP, and GPP_leaf (Figure 6). Similarly, at the daily timescale, the three models predicted a significant positive response of GPP_leaf to soil water content ($p < .05$), which was consistent with the observations (Figure 7). This suggests that, reproducing soil moisture in critical growing periods and the VWC-GPP_leaf relation can compensate for the poor estimates of LAI to a large extent, thus contributing the success of the three models in capturing GPP reductions in the drought years. Note that the simulated sensitivity (i.e., the slope of VWC-GPP relationship) by CLM and Biome-BGC was apparently lower than the observations, which in part explained the underestimation of GPP reduction in the drought years by these two models.

For the remaining three models (BEPS, CABLE and TECO), in addition to failure of capturing the VWC-LAI relation, they also failed to capture the VWC-GPP_leaf relation at both annual and daily scales, resulting in the failure of reproducing the observed VWC-GPP relationship (Figures 6 and 7).

3.4 | Effects of stomatal conductance and V_{cmax} on GPP variations

Since g_s and V_{cmax} are the key model parameters determining GPP_leaf, we further investigated the performance of models in simulating responses of g_s and V_{cmax} to soil water content. Apparently, all the three models (i.e., Biome-BGC, CLM and ORCHIDEE) that captured the observed VWC-GPP_leaf relationship with some

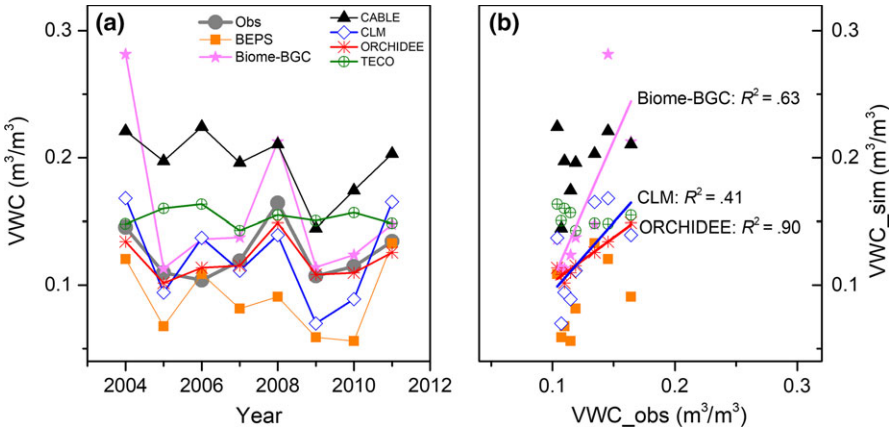

FIGURE 5 Data-model comparisons of interannual variations in VWC (0–30 cm). VWC was the mean of July to August (DOY 181-240). (a) Interannual variations in observed and modeled VWC. (b) Correlations between modeled and observed VWC. Only the fitted lines that are statistically significant at the level of 0.05 are shown [Colour figure can be viewed at wileyonlinelibrary.com]

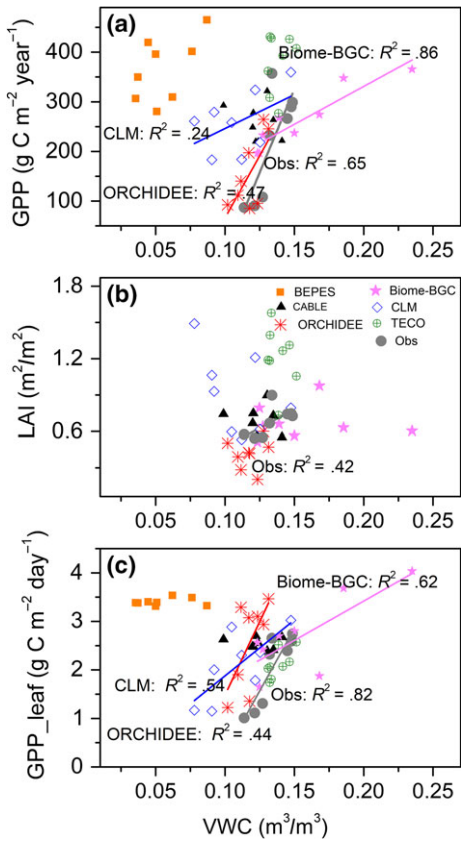

FIGURE 6 Correlations between average VWC in growing season and (a) annual GPP, (b) mean daily LAI in growing season, and (c) mean GPP_leaf of growing season for both observations and models. R^2 is the coefficient of determination of the linear relationships [Colour figure can be viewed at wileyonlinelibrary.com]

success also produced a significant correlation between g_s and VWC (Figure 8). Correspondingly, the models that failed to capture the VWC-GPP_leaf relation (BEPS, CABLE, and TECO) also failed to produce positive VWC-g_s relationship. In comparison, except CLM, which illustrated positive correlation between VWC and V_{cmax} when VWC was at median to lower levels, all the models simulated nonsignificant VWC-V_{cmax} correlation (Figure S5, $p > .05$). The above results suggest that stomatal conductance possibly dominated the response of GPP_leaf to variations in soil moisture in the models.

4 | DISCUSSION

4.1 | Interannual variations in GPP due to changes in water availability

We found that changes in VWC were the key reason causing the interannual variations in GPP in the temperate grassland. Especially, sharp reductions in GPP were detected in drought years (Figure 2). Our finding is consistent with previous studies, which showed that annual ecosystem carbon exchange and primary productivity were mainly determined by water availability in ecosystems under semiarid and arid climates (Guo et al., 2015; Knapp & Smith, 2001).

We found the reductions in LAI in drought years were smaller than that of GPP and GPP_leaf, and the R^2 between VWC and GPP_leaf was larger than that of VWC and LAI, suggesting that changes in GPP_leaf contributed more to the variance of annual GPP than LAI. This result is consistent with the processes of plant physiology, since changes in GPP_leaf (i.e., photosynthesis) is a first-order consequence and changes in LAI is a second-order consequence owing to changes in environmental conditions. Severe water stress can cause damage of leaf growth (Peters, Yao, Browning, & Rango, 2014) and trigger leaf senescence or even mortality of vegetation (Tan et al., 2013). However, before the threshold where water stress can produce permanent damage, LAI would remain relatively constant despite decline of GPP. This mechanism would be critical for the grassland species living in arid and semiarid environments, which have evolved to cope with frequent drought during growing seasons in the region.

Owing to the high within-year variations in soil water content, LAI also varied considerably during the growing seasons in some ecosystems, which contributed significantly to the observed IAV of GPP and poses another challenge for the present generation of models. For example, in a similar model-data intercomparison at a temperate grassland in Wyoming, USA, De Kauwe et al. (2017) found that the models failed because they did not reproduce the variation in greenness (a proxy of LAI) within each year as a function of soil

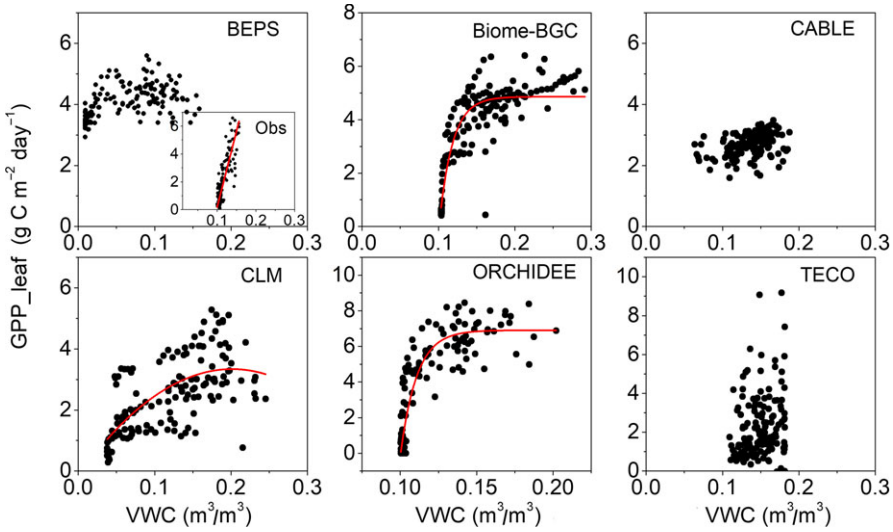

FIGURE 7 Correlations between daily VWC and GPP_leaf for both observations and models during the peak growing season (DOY 180-200). Only significant relationships at the level of 0.05 are shown [Colour figure can be viewed at wileyonlinelibrary.com]

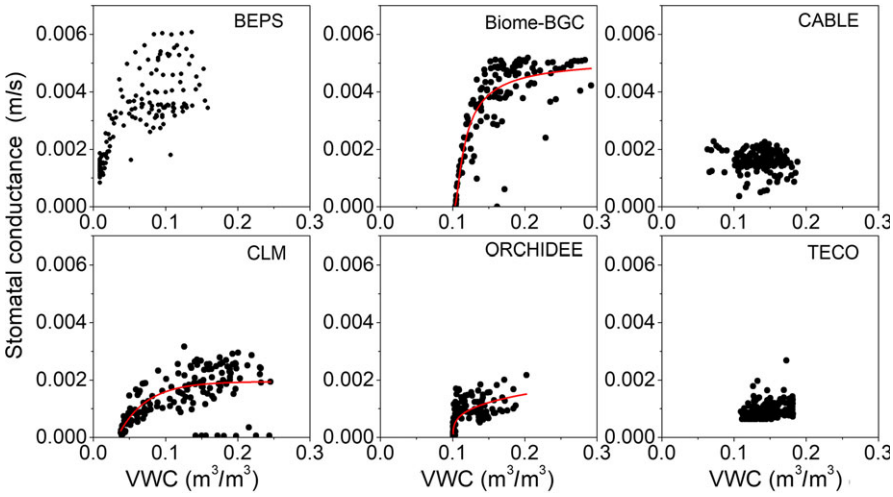

FIGURE 8 Correlations between daily g_s and VWC for participating models during day of year (DOY) 180-200 in all years. Only significant relationships ($p < .05$) are shown [Colour figure can be viewed at wileyonlinelibrary.com]

moisture availability. At our study site, we also detected a certain degree of temporary pauses of LAI increase during growing seasons when VWC fell low (Hao et al., 2010). However, in contrast with the large fluctuations of LAI due to changes in VWC at the site of De Kauwe et al. (2017), the seasonal LAI were relatively smooth and independent from the seasonal variations in soil water content.

In this study, GPP was calculated as the sum of NEP and R_{eco}. Since soil water content was used to estimate R_{eco}, and this may contributed to the observed annual GPP-VWC relationship. Note that the VWC at soil surface (at the depth of 5 cm) was used to estimate R_{eco}, but that of the average of rooting zone (0–30 cm) was used for investigating the GPP-VWC relation. Considering the contrast magnitudes and dynamics of soil moisture at different soil depths (Guo et al., 2015), the estimate of R_{eco} with VWC contributed minor to the annual GPP-VWC relationship.

4.2 | Uncertainties in simulating LAI

Our results indicate that, during the whole study period, the models with prescribed LAI (i.e., BEPS and CABLE) reproduced the interannual variations of the observed GPP well. In contrast, the models that yielded poor estimate of LAI predicted relatively larger biases of the observed interannual variations in GPP. These results highlight the importance of improving LAI simulation for predicting GPP in the grassland ecosystems (De Kauwe et al., 2017).

All the four prognostic models in our study failed to capture the interannual variations in LAI, as well as the VWC-LAI relationship in the grassland ecosystem, largely as a result of the large errors in representing the influences of available soil water on carbon allocation. Plant tends to optimally utilize changing resources by adjusting the fractions of carbon allocation in above- *vs.* below-ground compartments, e.g., more leaves when water is abundant and more roots when water stress occurs (Haverd et al., 2016). However, besides models employing a fixed ratio of carbon allocation to leaves and roots (e.g., Biome-BGC), the models using dynamic carbon allocation with changes in resources availability (e.g., ORCHIDEE and TECO) were still failed in predicting interannual LAI dynamics in response to VWC. This implies that the current parameterization scheme based on resource limitation failed to account for the impact of soil water content on carbon allocation, at least at annual time scale, which is

critical for simulating GPP in ecosystems under arid and semiarid environments.

Beside the uncertainty induced by imperfect carbon allocation schemes, the constant SLA used in the models may also contribute to the biased estimation of LAI. Observations show that SLA varies throughout the growing season (Tardieu, Granier, & Muller, 1999) as a result of varying nitrogen availability (Amanullah, Nawab, & Ali, 2013) and drought stress (Liu & Stutzel, 2004). A previous study found that constant SLA in models significantly contributed to the biases of modeled LAI (Drewniak, Song, Prell, Kotamarthi, & Jacob, 2013). Therefore, for improving models' performance in predicting the temporal variations in LAI, dynamic measurements of SLA and clarifying the controlling factors in various environmental conditions are needed.

4.3 | Uncertainties in simulating GPP_leaf

Our results highlight the importance of the physiological component, GPP_leaf in determining the interannual variations in GPP. The importance of plant physiological processes in regulating the spatiotemporal variations of GPP has been widely reported in recent years (Xia et al., 2016; Zhou et al., 2016). Owing to failing to reproduce the interannual variability in GPP_leaf, the models with prescribed LAI (i.e., BEPS and CABLE) underestimated the interannual variability in GPP (Figure 4). In contrast, because of the success of reproducing the interannual variations in GPP_leaf, the three models with prognostic LAI (i.e., Biome-BGC, CLM, and ORCHIDEE) captured the GPP reductions in drought years. This phenomenon is unexpected because a general view is that LAI overwhelmingly dominates the interannual variations in GPP (Duursma et al., 2009; Puma, Koster, & Cook, 2013). As we discussed above, however, changes in LAI is a consequence of changes in leaf photosynthesis. Thus, intuitively GPP_leaf should be more variable than LAI in response to soil water stress. This observation was not successfully captured by most of the six models.

The diverging performances on simulating GPP_leaf is also surprising since most models employ Farquhar's scheme (or its variants) to simulate leaf photosynthesis and thus the simulated GPP_leaf or at least the VWC-GPP_leaf relation should be similar among the six models. However, parameterization of stomatal conductance and V_{cmax} differ significantly among the six model, which may have contributed to the diverging responses of GPP_leaf to VWC by those models. Further analysis indicates that the models with acceptable performance on simulation of GPP_leaf also performed better in simulating VWC-GPP_leaf relation and VWC-g_s relation (Figures 6–8). This implies that the model capability in capturing g_s sensitivity to soil water content critically impacts on its ability in accurately simulating GPP_leaf prediction, thus GPP for the semiarid grassland.

The simulated g_s among the six models differed as much as fivefold, many factors, such as how the biochemical model of photosynthesis is parametrized, and coupling of g_s and photosynthesis, and their responses to environmental variable may contribute to the difference. Because of the dominant influences of soil water on all major processes, we focused on the VWC-g_s relationship, not the magnitude of g_s in our study. All the six models except CLM and ORCHIDEE explicitly include soil water stress functions on g_s (Table 1). However, models (e.g., BEPS, CABLE, and TECO) including a water scalar on g_s is till failed in reproducing the observed responses of g_s and GPP_leaf to VWC. Therefore, the water constraints in g_s models of BEPS, CABLE, and TECO has large model errors. Unfortunately, we did not successfully identify the underlying causes for the large errors in the modeled g_s in this study. This should be explored further in future studies.

4.4 | Uncertainties in simulating soil moisture

Soil water content was found to be the key factor driving the interannual variations in LAI and GPP_leaf at the grassland site. Only three models reproduced the observed interannual variations in VWC of the critical growth periods (Figure 5). Since the models used the same soil water-holding capacity and were driven by the same precipitation forcing, possible sources of the intermodel difference in VWC includes errors in the modeled ET, runoff, and vertical movement of soil moisture. All the models except TECO illustrated similar interannual variations in ET (mean R^2 of intermodel relationships was .75, Figure S6). For example, the R^2 of simulated ET by CABLE and ORCHIDEE was as high as .96, but very low for VWC by the two models ($R^2 = .25$, $p > .05$). This indicates that ET is not likely to be the dominant source of errors in the modeled VWC. It is possible that large errors resulted from different effective soil depths or vertical distribution of roots in soil (Table 1). Those differences will result in different estimates of runoff and VWC in the rooting zone. Further studies are warranted to investigate how changes of root distribution affect soil water profile in the rooting zone.

We also found that none of the six models were able to capture the observed interannual variation in mean VWC (and ET) of the whole growing seasons (Figure S4). Before July and August, vegetation cover was low, soil water evaporation accounted for most of ET in the grassland (Hu et al., 2009). Inaccurate simulation of soil evaporation in early growing seasons may have contributed to the errors in ET and VWC of the whole growing season. As also found by De Kauwe et al. (2017), the estimated soil evaporation for a temperate grassland can differ significantly among different models.

4.5 | Implications of the GPP component analysis framework for model improvements

In this study, we proposed a component analysis framework to identify the sources of model uncertainty on GPP prediction. The advantages of the framework lie in two aspects. First, the two components of GPP are relatively independent in model representations, i.e., LAI involved in carbon allocations and GPP_leaf mainly related with leaf-scale eco-physiological processes. Thus, the effects of these two subprocesses can be independently examined. Second, both GPP and LAI can be directly measured or derived conveniently using current technologies. These advantages can help address the

deficits of models in describing vegetation physiological *vs.* structural characteristics under environmental limitations. Therefore, our framework has the potential to facilitate future model intercomparison, benchmarking and optimization.

ACKNOWLEDGEMENTS

This study was jointly supported by National Key R&D Program of China (2017YFA0604801), the National Natural Science Foundation of China (Grant No. 31570437, 41730645, and 41371119), the Startup Foundation for Talented Scholars in South China Normal University (S82360), the Youth Innovation Research Team Project of LENOM, CAS (LENOM2016Q0004),the Youth Innovation Promotion Association, CAS (Grant No. 2015037), the Special-Funds of Scientific Research Programs of State Key Laboratory of Soil Erosion and Dryland Farming on the Loess Plateau (A314021403-C4 and A314021402-1703) and the Special-Fund of talents (Thousand Talents Program) in Northwest A&F University. The authors thank two anonymous reviewers for their insightful and constructive comments on our manuscript.

ORCID

Zhongmin Hu http://orcid.org/0000-0002-4801-5370
Hao Shi http://orcid.org/0000-0001-8250-0567
Shilong Piao http://orcid.org/0000-0001-8057-2292
Jianyang Xia http://orcid.org/0000-0001-5923-6665
Yanbin Hao http://orcid.org/0000-0001-6821-0395
Nianpeng He http://orcid.org/0000-0002-0458-5953

REFERENCES

Agren, G. I., Wetterstedt, J. A. M., & Billberger, M. F. K. (2012). Nutrient limitation on terrestrial plant growth-modeling the interaction between nitrogen and phosphorus. *New Phytologist*, *194*, 953–960. https://doi.org/10.1111/j.1469-8137.2012.04116.x

Ahlstrom, A., Raupach, M. R., Schurgers, G., Smith, B., Arneth, A., Jung, M., … Zeng, N. (2015). The dominant role of semi-arid ecosystems in the trend and variability of the land CO_2 sink. *Science*, *348*, 895–899. https://doi.org/10.1126/science.aaa1668

Amanullah, M. J. H., Nawab, K., & Ali, A. (2013). Response of specific leaf area (SLA), leaf area index (LAI) and leaf area ratio (LAR) of Maize (Zea mays L.) to plant density, rate and timing of nitrogen application. *World Applied Sciences Journal*, *2*, 235–243.

Ball, J. T., Woodrow, I. E., & Berry, J. A. (1987). A model predicting stomatal conductance and its contribution to the control of photosynthesis under different environmental conditions. In J. Biggins (Ed.), *Progress in photosynthesis research* (pp. 221–224). Dordrecht, the Netherlands: Springer Netherlands. https://doi.org/10.1007/978-94-017-0519-6

Best, M. J., Abramowitz, G., Johnson, H. R., Pitman, A. J., Balsamo, G., Boone, A., … Vuichard, N. (2015). The plumbing of land surface models: Benchmarking model performance. *Journal of Hydrometeorology*, *16*, 1425–1442. https://doi.org/10.1175/JHM-D-14-0158.1

Chen, J. M., Liu, J., Cihlar, J., & Goulden, M. L. (1999). Daily canopy photosynthesis model through temporal and spatial scaling for remote sensing applications. *Ecological Modelling*, *124*, 99–119. https://doi.org/10.1016/S0304-3800(99)00156-8

Collatz, G. J., Ball, J. T., Grivet, C., & Berry, J. A. (1991). Physiological and environmental regulation of stomatal conductance, photosynthesis and transpiration: A model that includes a laminar boundary layer. *Agricultural and Forest Meteorology*, *54*, 107–136. https://doi.org/10.1016/0168-1923(91)90002-8

Collatz, G. J., Ribascarbo, M., & Berry, J. A. (1992). Coupled photosynthesis–stomatal conductance model for leaves of C4 plants. *Australian Journal of Plant Physiology*, *19*, 519–538. https://doi.org/10.1071/PP9920519

Craine, J. M., & Brunsell, N. A. (2012). Timing of climate variability and grassland productivity. *Proceedings of the National Academy of Sciences of the United States of America*, *109*, 3401–3405. https://doi.org/10.1073/pnas.1118438109

Cramer, W., Bondeau, A., Woodward, F. I., Prentice, I. C., Betts, R. A., Brovkin, V., … Young-Molling, C. (2001). Global response of terrestrial ecosystem structure and function to CO_2 and climate change: Results from six dynamic global vegetation models. *Global Change Biology*, *7*, 357–373. https://doi.org/10.1046/j.1365-2486.2001.00383.x

Dai, A. (2013). Increasing drought under global warming in observations and models. *Nature Climate Change*, *3*, 52–58. https://doi.org/10.1038/nclimate1633

De Kauwe, M. G., Medlyn, B. E., Walker, A. P., Zaehle, S., Asao, S., Guenet, B., … Norby, R. J. (2017). Challenging terrestrial biosphere models with data from the long-term multifactor Prairie Heating and CO2 Enrichment experiment. *Global Change Biology*, *23*, 3623–3645. https://doi.org/10.1111/gcb.13643

De Kauwe, M. G., Zhou, S., Medlyn, B. E., Pitman, A. J., Wang, Y., Duursma, R. A., & Prentice, I. C. (2015). Do land surface models need to include differential plant species responses to drought? Examining model predictions across a mesic-xeric gradient in Europe. *Biogeosciences*, *12*, 7503–7518. https://doi.org/10.5194/bg-12-7503-2015

Drewniak, B., Song, J., Prell, J., Kotamarthi, V. R., & Jacob, R. (2013). Modeling agriculture in the Community Land Model. *Geoscientific Model Development*, *6*, 495–515. https://doi.org/10.5194/gmd-6-495-2013

Duursma, R. A., Kolari, P., Peramaki, M., Pulkkinen, M., Makela, A., Nikinmaa, E., … Vesala, T. (2009). Contributions of climate, leaf area index and leaf physiology to variation in gross primary production of six coniferous forests across Europe: A model-based analysis. *Tree Physiology*, *29*, 621–639. https://doi.org/10.1093/treephys/tpp010

Farquhar, G. D., Von Caemmerer, S., & Berry, J. A. (1980). A biochemical model of photosynthetic CO_2 assimilation in leaves of C3 species. *Planta*, *149*, 78–90. https://doi.org/10.1007/BF00386231

Friedlingstein, P., Cox, P., Betts, R., Bopp, L., von Bloh, W., Brovkin, V., … Zeng, N. (2006). Climate–carbon cycle feedback analysis: Results from the C^4MIP model intercomparison. *Journal of Climate*, *19*, 3337–3353. https://doi.org/10.1175/JCLI3800.1

Guo, Q., Hu, Z., Li, S., Yu, G., Sun, X., Zhang, L., … Zhao, W. (2015). Contrasting responses of gross primary productivity to precipitation events in a water-limited and a temperature-limited grassland ecosystem. *Agricultural and Forest Meteorology*, *214–215*, 169–177. https://doi.org/10.1016/j.agrformet.2015.08.251

Hao, Y., Wang, Y., Mei, X., Cui, X., Zhou, X., & Huang, X. (2010). The sensitivity of temperate steppe CO_2 exchange to the quantity and timing of natural interannual rainfall. *Ecological Informatics*, *5*(3), 222–228. https://doi.org/10.1016/j.ecoinf.2009.10.002

Haverd, V., Smith, B., Raupach, M., Briggs, P., Nieradzik, L., Beringer, J., … Cleverly, J. (2016). Coupling carbon allocation with leaf and root phenology predicts tree-grass partitioning along a savanna rainfall gradient. *Biogeosciences*, *13*, 761–779. https://doi.org/10.5194/bg-13-761-2016

Hu, Z., Yu, G., Fu, Y., Sun, X., Li, Y., Shi, P., ... Zheng, Z. (2008). Effects of vegetation control on ecosystem water use efficiency within and among four grassland ecosystems in China. *Global Change Biology*, *14*, 1609–1619. https://doi.org/10.1111/j.1365-2486.2008.01582.x

Hu, Z., Yu, G., Zhou, Y., Sun, X., Li, Y., Shi, P., ... Li, S. (2009). Partitioning of evapotranspiration and its controls in four grassland ecosystems: Application of a two-source model. *Agricultural and Forest Meteorology*, *149*, 1410–1420. https://doi.org/10.1016/j.agrformet.2009.03.014

Huang, J., Guan, X., & Ji, F. (2012). Enhanced cold-season warming in semi-arid regions. *Atmospheric Chemistry and Physics*, *12*, 5391–5398. https://doi.org/10.5194/acp-12-5391-2012

Jackson, R. B., Canadell, J., Ehleringer, J. R., Mooney, H. A., Sala, O. E., & Schulze, E. D. (1996). A global analysis of root distributions for terrestrial biomes. *Oecologia*, *108*, 389–411. https://doi.org/10.1007/BF00333714

Jarvis, P. G. (1976). The interpretation of the variations in leaf water potential and stomatal conductance found in canopies in the field. *Philosophical Transactions of the Royal Society B*, *273*, 593–610. https://doi.org/10.1098/rstb.1976.0035

Knapp, A. K., & Smith, M. D. (2001). Variation among biomes in temporal dynamics of aboveground primary production. *Science*, *291*, 481–484. https://doi.org/10.1126/science.291.5503.481

Kowalczyk, E. A., Wang, Y. P., & Law, E. M. (2006). *The CSIRO atmospheric biosphere land exchnage (CABLE) model for use in climate models and as an offline model*. Tech. Pap. 013, CSIRO Mar. and Atmos. Res., Aspendale, Vic., Australia.

Krinner, G., Viovy, N., de Noblet-Ducoudré, N., Ogée, J., Polcher, J., Friedlingstein, P., ... Prentice, I. C. (2005). A dynamic global vegetation model for studies of the coupled atmosphere-biosphere system. *Global Biogeochemical Cycles*, *19*(1).

Leuning, R. (1995). A critical appraisal of a combined stomatal-photosynthesis model for C3 plants. *Plant Cell and Environment*, *18*, 339–355. https://doi.org/10.1111/j.1365-3040.1995.tb00370.x

Li, L., Wang, Y., Arora, V. K., Eamus, D., Shi, H., Li, J., ... Yu, Q. (2018). Evaluating global land surface models in CMIP5: Analysis of ecosystem water- and light-use efficiencies and rainfall partitioning. *Journal of Climate*, *31*, 2995–3008. https://doi.org/10.1175/JCLI-D-16-0177.1

Liu, F., & Stutzel, H. (2004). Biomass partitioning, specific leaf area, and water use efficiency of vegetable amaranth (Amaranthus spp.) in response to drought stress. *Scientia Horticulturae*, *102*, 15–27. https://doi.org/10.1016/j.scienta.2003.11.014

Luo, X., Liang, X., & Mccarthy, H. R. (2013). VIC+ for water-limited conditions: A study of biological and hydrological processes and their interactions in soil-plant-atmosphere continuum. *Water Resources Research*, *49*, 7711–7732. https://doi.org/10.1002/2012WR012851

Luo, Y. Q., Randerson, J. T., Abramowitz, G., Bacour, C., Blyth, E., Carvalhais, N., ... Zhou, X. H. (2012). A framework for benchmarking land models. *Biogeosciences*, *9*(10), 3857–3874. https://doi.org/10.5194/bg-9-3857-2012

Murray-Tortarolo, G., Anav, A., Friedlingstein, P., Sitch, S., Piao, S., Zhu, Z., ... Zeng, N. (2013). Evaluation of land surface models in reproducing satellite-derived LAI over the high-latitude northern hemisphere. Part I: Uncoupled DGVMs. *Remote Sensing*, *5*, 4819–4838. https://doi.org/10.3390/rs5104819

Oleson, K. W., Lawrence, D. M., Bonan, G. B., Flanner, M. G., Kluzek, E., Lawrence, P. J., ... Zeng, X. (2010). *Technical description of version 4.0 of the community land model (CLM)*. NCAR Tech. Note, NCAR/TN-461 + STR., National Centre for Atmospheric Research, Boulder, Colorado.

Peters, D. P. C., Yao, J., Browning, D. M., & Rango, A. (2014). Mechanisms of grass response in grasslands and shrublands during dry or wet periods. *Oecologia*, *174*, 1323–1334. https://doi.org/10.1007/s00442-013-2837-y

Piao, S., Sitch, S., Ciais, P., Friedlingstein, P., Peylin, P., Wang, X., ... Zeng, N. (2013). Evaluation of terrestrial carbon cycle models for their response to climate variability and to CO_2 trends. *Global Change Biology*, *19*, 2117–2132. https://doi.org/10.1111/gcb.12187

Prentice, I. C., Liang, X., Medlyn, B. E., & Wang, Y. P. (2015). Reliable, robust and realistic: The three R's of next-generation land-surface modelling. *Atmospheric Chemestry and Physics*, *15*, 5987–6005. https://doi.org/10.5194/acp-15-5987-2015

Puma, M. J., Koster, R. D., & Cook, B. I. (2013). Phenological versus meteorological controls on land-atmosphere water and carbon fluxes. *Journal of Geophysical Research*, *118*, 14–29.

Reich, P. B., Hobbie, S. E., Lee, T., Ellsworth, D. S., West, J. B., Tilman, D., ... Trost, J. (2006). Nitrogen limitation constrains sustainability of ecosystem response to CO_2. *Nature*, *440*, 922–925. https://doi.org/10.1038/nature04486

Restrepocoupe, N., Levine, N. M., Christoffersen, B. O., Albert, L. P., Wu, J., Costa, M. H., ... Saleska, S. R. (2016). Do dynamic global vegetation models capture the seasonality of carbon fluxes in the Amazon basin? A data-model intercomparison *Global Change Biology*, *23*(1), 191–208.

Rotenberg, E., & Yakir, D. (2010). Contribution of semi-arid forests to the climate system. *Science*, *327*, 451–454. https://doi.org/10.1126/science.1179998

Safriel, U., & Adeel, Z. (2005). *Dryland systems*. Washington, DC: Island Press.

Smith, W. K., Reed, S. C., Cleveland, C. C., Ballantyne, A. P., Anderegg, W. R. L., Wieder, W. R., ... Running, S. W. (2016). Large divergence of satellite and earth system model estimates of global terrestrial CO_2 fertilization. *Nature Climate Change*, *6*, 306–310. https://doi.org/10.1038/nclimate2879

Tan, Z. H., Cao, M., Yu, G. R., Tang, J. W., Deng, X. B., Song, Q. H., ... Zhang, Y. P. (2013). High sensitivity of a tropical rainforest to water variability: Evidence from 10 years of inventory and eddy flux data. *Journal of Geophysical Research: Atmospheres*, *118*(16), 9393–9400.

Tardieu, F., Granier, C., & Muller, B. (1999). Modelling leaf expansion in a fluctuating environment : are changes in specific leaf area a consequence of changes in expansion rate ? *New Phytologist*, *143*, 33–43. https://doi.org/10.1046/j.1469-8137.1999.00433.x

Thornton, P. E., Law, B. E., Gholz, H. L., Clark, K. L., Falge, E., Ellsworth, D. S., ... Sparks, J. P. (2002). Modeling and measuring the effects of disturbance history and climate on carbon and water budgets in evergreen needleleaf forests. *Agricultural and Forest Meteorology*, *113*, 185–222. https://doi.org/10.1016/S0168-1923(02)00108-9

Thornton, P. E., & Zimmermann, N. E. (2007). An improved canopy integration scheme for a land surface model with prognostic canopy structure. *Journal of Climate*, *20*, 3902–3923. https://doi.org/10.1175/JCLI4222.1

Wang, Y. P., Kowalczyk, E., Leuning, R., Abramowitz, G., Raupach, M. R., Pak, B., ... Luhar, A. (2011). Diagnosing errors in a land surface model (CABLE) in the time and frequency domains. *Journal of Geophysical Research*, *116*(G1).

Weng, E., & Luo, Y. (2008). Soil hydrological properties regulate grassland ecosystem responses to multifactor global change: A modeling analysis. *Journal of Geophysical Research*, *113*(G3).

White, M. A., Thornton, P. E., Running, S. W., & Nemani, R. R. (2000). Parameterization and sensitivity analysis of the BIOME–BGC terrestrial ecosystem model: Net primary production controls. *Earth Interactions*, *4*, 1–85. https://doi.org/10.1175/1087-3562(2000)004<0003:PASAOT>2.0.CO;2

Wilcox, K. R., Fischer, J. C., Muscha, J. M., Petersen, M. K., & Knapp, A. K. (2015). Contrasting above- and belowground sensitivity of three Great Plains grasslands to altered rainfall regimes. *Global Change Biology*, *21*, 335–344. https://doi.org/10.1111/gcb.12673

Xia, J., Luo, Y., Wang, Y.-P., & Hararuk, O. (2013). Traceable components of terrestrial carbon storage capacity in biogeochemical models. *Global Change Biology*, *19*, 2104–2116. https://doi.org/10.1111/gcb.12172

Xia, J., McGuire, A. D., Lawrence, D., Burke, E., Chen, G., Chen, X., … Luo, Y. (2017). Terrestrial ecosystem model performance in simulating productivity and its vulnerability to climate change in the northern permafrost region. *Journal of Geophysical Research Biogeosciences*, *122*, 430–446. https://doi.org/10.1002/2016JG003384

Xia, J., Niu, S., Ciais, P., Janssens, I. A., Chen, J., Ammann, C., … Luo, Y. (2016). Joint control of terrestrial gross primary productivity by plant phenology and physiology. *Proceedings of the National Academy of Sciences of the United States of America*, *112*(9), 2788–2793.

Yu, G. R., Wen, X. F., Sun, X. M., Tanner, B. D., Lee, X., & Chen, J. Y. (2006). Overview of ChinaFLUX and evaluation of its eddy covariance measurement. *Agricultural and Forest Meteorology*, *137*, 125–137. https://doi.org/10.1016/j.agrformet.2006.02.011

Zaehle, S., Medlyn, B. E., De Kauwe, M. G., Walker, A. P., Dietze, M. C., Hickler, T., … Norby, R. J. (2014). Evaluation of 11 terrestrial carbon–nitrogen cycle models against observations from two temperate Free-Air CO_2 Enrichment studies. *New Phytologist*, *202*, 803–822. https://doi.org/10.1111/nph.12697

Zhou, S., Zhang, Y., Caylor, K. C., Luo, Y., Ciais, P., Huang, Y., & Wang, G. (2016). Explaining inter-annual variability of gross primary productivity fromplant phenology and physiology. *Agricultural and Forest Meteorology*, *226–227*, 246–256. https://doi.org/10.1016/j.agrformet.2016.06.010

SUPPORTING INFORMATION

Additional supporting information may be found online in the Supporting Information section at the end of the article.

How to cite this article: Hu Z, Shi H, Cheng K, et al. Joint structural and physiological control on the interannual variation in productivity in a temperate grassland: A data-model comparison. *Glob Change Biol*. 2018;24:2965–2979. https://doi.org/10.1111/gcb.14274